

# Diffusion Models under Alternative Noise: Simplified Analysis and Sensitivity

Juhyeok Choi\*

Chenglin Fan†

## Abstract

Diffusion models, typically formulated as discretizations of stochastic differential equations (SDEs), have achieved state-of-the-art performance in generative tasks. However, their theoretical analysis often involves complex proofs. In this work, we present a simplified framework for analyzing the Euler–Maruyama discretization of variance-preserving SDEs (VP-SDEs). Using Grönwall’s inequality, we derive a convergence rate of  $O(T^{-1/2})$  under standard Lipschitz assumptions, streamlining prior analyses. We then demonstrate that the standard Gaussian noise can be replaced by computationally cheaper discrete random variables (e.g., Rademacher) without sacrificing this convergence guarantee, provided the mean and variance are matched. Our experiments validate this theory, showing that (i) discrete noise achieves sample quality comparable to Gaussian noise provided the variance is matched correctly, and (ii) performance degrades if the noise variance is scaled incorrectly.

## 1 INTRODUCTION

Diffusion models are a class of generative models that have recently achieved state-of-the-art performance in tasks such as image synthesis, audio generation, and molecular design. Originally introduced as a probabilistic framework [Sohl-Dickstein et al., 2015], their modern success was catalyzed by significant practical and theoretical advancements, particularly the formulation as a denoising process [Ho et al., 2020] and their unification with score-based models through a common stochastic differential equation (SDE) framework [Song et al., 2021b]. Inspired by non-equilibrium thermodynamics, these models learn to reverse a gradual noising process, transforming pure noise into structured data through a series of denoising steps.

The core idea behind diffusion models is to model the data distribution by simulating a Markovian forward process that incrementally adds Gaussian noise to the data, eventually destroying all structure. A neural network is then trained to approximate the reverse process — learning to recover clean data from noisy observations. Once trained, the model can generate new samples by starting from random noise and iteratively applying the learned denoising steps (Sohl-Dickstein et al. [2015], Ho et al. [2020]).

Compared to other generative approaches such as Generative Adversarial Networks (GANs; Goodfellow et al., 2014) and Variational Autoencoders (VAEs; Kingma and Welling, 2014), diffusion models are often more stable to train and produce higher-quality samples, albeit with slower generation speed due to their iterative nature. Recent advances have focused on mitigating these limitations. For instance, Denoising Diffusion Implicit Models (DDIM) introduced a more efficient, non-Markovian sampling process [Song et al., 2021a], while techniques like classifier-free guidance

\*Seoul National University, Seoul, 08826, South Korea. [wrons13@snu.ac.kr](mailto:wrons13@snu.ac.kr)

†Seoul National University, Seoul, 08826, South Korea. [fan Chenglin@snu.ac.kr](mailto:fan Chenglin@snu.ac.kr). **Corresponding author.**

improved sample quality and control without needing an external classifier [Ho et al., 2022a]. More recently, consistency models have enabled high-quality, one-step generation by mapping any point on the SDE trajectory directly to the origin [Song et al., 2023].

Diffusion models have quickly become a central tool in generative AI research, offering both strong theoretical grounding and impressive empirical results across a wide range of applications. These include text-to-image generation through models like DALL-E 2, Imagen, and the highly efficient Latent Diffusion Models [Ramesh et al., 2022, Saharia et al., 2022], audio synthesis [Kong et al., 2021], molecular and protein design [Trippe et al., 2022, Watson et al., 2023], video generation [Ho et al., 2022b], and medical imaging [Wolleb et al., 2022].

The theoretical foundations of diffusion models have been established through their connection to SDEs [Song et al., 2021b]. Recent work has initiated rigorous analyses of sampling complexity. For general input distributions, Benton et al. [2023] obtained a bound scaling linearly with the dimension  $d$ , requiring  $\mathcal{O}(d/\varepsilon^2)$  iterations. Li et al. [2024] refined this in the regime  $T/\log^5 T = \Omega(d^2)$ , reducing the complexity to  $\mathcal{O}(d/\varepsilon)$ . Under additional smoothness assumptions, the iteration complexity further improves to  $\min\{d, d^{2/3}L^{1/3}, d^{1/3}L\} \cdot \varepsilon^{-2/3}$  [Jiao and Li, 2025], where  $L$  denotes a relaxed Lipschitz constant of the score function. Other directions include the study of quantized and low-precision noise [Xiao et al., 2022], though without convergence guarantees, as well as polynomial-rate results for more general settings [Chen et al., 2023b, Lee et al., 2023, Li et al., 2023, Chen et al., 2023a]. For surveys of recent progress, see Yang et al. [2023], Tang and Zhao [2024].

**Contributions.** In this paper, we make the following contributions:

- **Simplified analysis.** We analyze the reverse-time variance-preserving SDE (VP-SDE) using a time-rescaled formulation and Grönwall’s inequality, yielding a cleaner and more accessible proof structure.
- **Noise substitution.** We show that the Gaussian noise used in the reverse sampling process can be replaced with simpler, computationally cheaper discrete noise distributions (e.g., Rademacher) while preserving the same convergence rate. We prove that the error incurred by this substitution is of the same order as the Euler–Maruyama discretization error, provided the alternative noise matches the first two moments of the Gaussian (zero mean and unit variance).
- **Experiments.** We empirically demonstrate that symmetric discrete noise achieves sample quality nearly indistinguishable from Gaussian noise, thereby validating our theoretical findings.

## 2 PRELIMINARIES

### 2.1 Grönwall’s Inequality

Grönwall’s inequality (Gronwall [1919]) is a fundamental tool for establishing bounds in the analysis of differential equations and numerical schemes. It provides a powerful method to bound a function that satisfies a certain type of integral inequality.

**Theorem 2.1** (Continuous version of Grönwall’s Inequality). *Let  $a \geq 0$  and  $b, u : [0, T] \rightarrow \mathbb{R}_+$  be continuous functions. If*

$$u(t) \leq a + \int_0^t b(s)u(s)ds,$$

then

$$u(T) \leq a \exp \left( \int_0^T b(t) dt \right).$$

A useful corollary provides a discrete analogue of this result for non-negative sequences, which is essential for analyzing iterative methods.

**Corollary 2.2** (Discrete version of Grönwall’s Inequality). *Let  $a \geq 0$  and  $\{u_n\}, \{b_n\}$  be non-negative sequences. If*

$$u_n \leq a + \sum_{k=0}^{n-1} b_k u_k,$$

for all  $n \in \mathbb{N}$ , then

$$u_n \leq a \left( 1 + \sum_{k=0}^{n-1} b_k \prod_{j=k+1}^{n-1} (1 + b_j) \right).$$

## 2.2 Diffusion Models

Diffusion models are generative models that transform a simple noise distribution into a complex data distribution by simulating a time-reversed stochastic process. The forward process (also called the diffusion process) gradually adds noise to data, while the reverse process (also called the generative or sampling process) aims to recover data from pure noise.

**Forward Process.** Let  $X_0 \sim p_{\text{data}}$  be a sample from the data distribution. The forward process  $\{X_t\}_{t \in [0,1]}$  evolves according to the SDE:

$$dX_t = -\frac{1}{2}\beta(t)X_t dt + \sigma(t) dW_t,$$

where  $W_t$  is a standard Wiener process,  $\beta(t) : [0, 1] \rightarrow \mathbb{R}_+$  is a non-decreasing noise schedule, and we define  $\sigma(t) := \sqrt{\beta(t)}$  following the Variance-Preserving (VP) SDE formulation in (Song et al. [2021b]). This process transforms the data distribution into a tractable noise distribution (typically  $\mathcal{N}(0, I)$ ) as  $t \rightarrow 1$ .

**Reverse Process.** By results from stochastic calculus (e.g., Anderson’s time-reversal of diffusions), the reverse-time process  $\{\bar{X}_t\}_{t \in [0,1]}$  also follows an SDE:

$$d\bar{X}_t = \left( -\frac{1}{2}\beta(t)\bar{X}_t - \beta(t)\nabla_x \log p_t(\bar{X}_t) \right) dt + \sqrt{\beta(t)}d\bar{W}_t,$$

where  $\bar{W}_t$  is a reverse-time Wiener process and  $p_t$  is the marginal distribution of  $X_t$  in the forward process.

In practice, the score function  $\nabla_x \log p_t(x)$  is intractable, so it is approximated by a neural network trained to predict either the score or the noise added during the forward process. In particular, Denoising Diffusion Probabilistic Models (DDPM) (Ho et al. [2020]) use a parameterized

model  $\epsilon_\theta(x, t)$  to estimate the noise in the forward process. Plugging this into the reverse SDE leads to the following approximate generative process:

$$d\bar{X}_t = \left( \frac{\beta(t)}{\sigma_t} \epsilon_\theta(\bar{X}_t, t) - \frac{\beta(t)}{2} \bar{X}_t \right) dt + \sqrt{\beta(t)} d\bar{W}_t,$$

which is the SDE we analyze in the following section. Our goal is to quantify the error when simulating this reverse-time process using the Euler–Maruyama scheme.

### 2.3 Prior Works on Non-Gaussian Diffusion

While the standard diffusion framework relies heavily on Gaussian noise, recent works have explored alternative noise distributions to extend modeling capabilities. One line of research focuses on heavy-tailed distributions to better capture outliers in real-world data. For instance, Denoising Lévy Probabilistic Models (DLPM) [Yoon et al., 2023] and Heavy-Tailed Diffusion Models [Pandey et al., 2025] replace Gaussian noise with  $\alpha$ -stable or Student- $t$  distributions, demonstrating improved performance on heavy-tailed datasets where Gaussian priors fail. Similarly, Gamma Diffusion Models [Nachmani and Wolf, 2021] utilize Gamma noise to better fit data with specific structural constraints.

Another direction generalizes the diffusion process beyond noise entirely. Approaches like Cold Diffusion [Bansal et al., 2022] and Soft Diffusion [Daras et al., 2022] demonstrate that generative behavior can emerge from deterministic degradations, such as blurring or masking, proving that Gaussian randomness is not strictly necessary for the generative mechanism.

**Our Contribution.** Unlike these works, which fundamentally alter the forward process or data assumptions, our approach retains the standard VP-SDE formulation but targets *computational efficiency in the sampling solver*. While Xiao et al. [Xiao et al., 2022] explored discrete denoising for low-precision hardware, they lacked rigorous convergence guarantees for the sampling SDE. We bridge this gap by proving that computationally cheaper discrete noise (e.g., Rademacher) can substitute Gaussian noise in the Euler-Maruyama scheme without sacrificing the  $\mathcal{O}(T^{-1/2})$  strong convergence rate, provided the first two moments are matched.

## 3 Proposed Method

### 3.1 Discretizing the Reverse-Time SDE via Euler–Maruyama

DDPM can be considered as a discretization of the reverse-time VP-SDE

$$d\bar{X}_t = \left( \frac{\beta(t)}{\sigma_t} \epsilon_\theta(\bar{X}_t, t) - \frac{\beta(t)}{2} \bar{X}_t \right) dt + \sqrt{\beta(t)} d\bar{W}_t.$$

To facilitate the analysis of the discretization error over a fixed interval, we re-parameterize the time variable from  $t \in [0, T]$  to  $\tau \in [0, 1]$  via the transformation  $\tau = t/T$ , where  $T$  is the number of timestep of DDPM. This normalization clarifies the step-size dependency. We obtain

$$\begin{aligned} d\bar{X}_\tau &= T \left( \frac{\beta(t)}{\sigma_t} \epsilon_\theta(\bar{X}_\tau, t) - \frac{\beta(t)}{2} \bar{X}_\tau \right) d\tau + \sqrt{T} \sqrt{\beta(t)} d\bar{W}_\tau \\ &= b(\bar{X}_\tau, \tau) d\tau + \sigma(\tau) d\bar{W}_\tau. \end{aligned}$$

The Euler-Maruyama discretization can be written as

$$\bar{X}_\tau^{(h)} = \bar{X}_{sh}^{(h)} + b(\bar{X}_{sh}, sh) (\tau - sh) + \sigma(sh) (\bar{W}_\tau - \bar{W}_{sh})$$

where  $\tau \in [(s-1)h, sh]$ . Here,  $h$  denotes the time interval, which equals  $1/T$ . With Lipschitz assumptions, we obtain that Euler-Maruyama discretization has the strong convergence rate of order  $1/2$ .

**Theorem 3.1.** *Suppose there exists  $k > 0$  such that*

$$\begin{aligned} |b(t, x) - b(s, y)| + |\sigma(t) - \sigma(s)| &\leq k \left( |x - y| + |t - s|^{1/2} \right), \\ |b(t, x)| + |\sigma(t)| &\leq k \end{aligned}$$

for all time  $t, s$  and objectives  $x, y$ . Then there exists  $c = c(k, x) > 0$  such that

$$\left( \mathbb{E} \left[ \sup_{0 \leq t \leq 1} \left| \overline{X}_t^{(h)} - \overline{X}_t \right|^2 \right] \right)^{1/2} \leq ch^{1/2}.$$

*Proof.* Let  $[s] = \lfloor s/h \rfloor h$  denote the start of the discretization interval containing  $s$ . Then

$$\overline{X}_\tau^{(h)} - \overline{X}_\tau = \int_\tau^1 \underbrace{b\left(\overline{X}_{[s]}^{(h)}, [s]\right) - b\left(\overline{X}_s^{(h)}, s\right)}_{=A} ds + \int_\tau^1 \underbrace{b\left(\overline{X}_s^{(h)}, s\right) - b\left(\overline{X}_s, s\right)}_{=B} ds + \int_\tau^1 \underbrace{\sigma([s]) - \sigma(s)}_{=C} d\overline{W}_s.$$

Here, note that

$$\mathbb{E} [|A|^2] \leq k^2 \left( |s - [s]|^{1/2} + \mathbb{E} \left[ \left| \overline{X}_s^{(h)} - \overline{X}_{[s]}^{(h)} \right| \right] \right)^2 \leq 2k^2 \left( |s - [s]| + \mathbb{E} \left[ \left| \overline{X}_s^{(h)} - \overline{X}_{[s]}^{(h)} \right|^2 \right] \right),$$

$$\mathbb{E} [|B|^2] \leq k^2 \mathbb{E} \left[ \left| \overline{X}_s^{(h)} - \overline{X}_s \right|^2 \right],$$

$$\mathbb{E} [|C|^2] \leq k^2 |s - [s]|.$$

By Jensen's inequality, we have

$$\begin{aligned} \mathbb{E} \left[ \sup_{x \leq \tau \leq 1} \left| \int_\tau^1 A ds \right|^2 \right] &\leq (1-x) \int_x^1 \mathbb{E} [|A|^2] ds, \\ \mathbb{E} \left[ \sup_{x \leq \tau \leq 1} \left| \int_\tau^1 B ds \right|^2 \right] &\leq (1-x) \int_x^1 \mathbb{E} [|B|^2] ds, \end{aligned}$$

Also, by Doob's maximal inequality, we have

$$\mathbb{E} \left[ \sup_{x \leq \tau \leq 1} \left| \int_\tau^1 \sigma([s]) - \sigma(s) d\overline{W}_s \right|^2 \right] \leq 4\mathbb{E} \left[ \int_x^1 |\sigma([s]) - \sigma(s)|^2 ds \right].$$

Now, let

$$m(x) = \mathbb{E} \left[ \sup_{x \leq \tau \leq 1} \left| \overline{X}_\tau^{(h)} - \overline{X}_\tau \right|^2 \right].$$

Then

$$\begin{aligned} m(x) &\leq 4 \left( (1-x) \int_x^1 \mathbb{E} [|A|^2] ds + (1-x) \int_x^1 \mathbb{E} [|B|^2] ds + 4 \int_x^1 \mathbb{E} [|C|^2] ds \right) \\ &\leq 40k^2 \int_x^1 |s - [s]| + \mathbb{E} \left[ \left| \overline{X}_s^{(h)} - \overline{X}_{[s]}^{(h)} \right| \right] ds + 20k^2 \int_x^1 \mathbb{E} \left[ \left| \overline{X}_s^{(h)} - \overline{X}_s \right|^2 \right] ds \\ &\leq 40k^2 \int_x^1 ch(1+h) ds + 60k^2 \int_x^1 m(s) ds. \end{aligned}$$

Hence, for some  $c > 0$ ,

$$m(x) \leq ch + c \int_x^1 m(s) ds.$$

Applying Grönwall’s inequality, we obtain

$$m(x) \leq che^{c(1-x)} \leq che^c.$$

□

### 3.2 Noise Substitution in Diffusion Models

In the Euler–Maruyama discretization, the Gaussian noise term can be replaced by a discrete random variable with the same mean and variance. Specifically, in the time-changed Euler–Maruyama scheme, the update rule is

$$\overline{X}_{\tau-h}^{(h)} = \overline{X}_{\tau}^{(h)} - b\left(\overline{X}_{\tau}^{(h)}, \tau\right)h - \sigma(\tau)B_h, \quad B_h \sim \mathcal{N}(0, h).$$

We consider replacing the Gaussian noise  $B_h$  with a scaled discrete random variable  $\sqrt{h}E$ , where  $E$  has zero mean and unit variance:

$$\overline{X}'_{\tau-h}{}^{(h)} = \overline{X}'_{\tau}{}^{(h)} - b\left(\overline{X}'_{\tau}{}^{(h)}, \tau\right)h - \sigma(\tau)\sqrt{h}E.$$

The primary motivation for this substitution lies in the computational overhead of random number generation (RNG) on hardware. Standard Gaussian sampling typically relies on algorithms such as the Box-Muller transform or the Ziggurat method. These approaches often require evaluating transcendental functions (e.g., logarithms, square roots, and trigonometric functions) or involve rejection sampling loops that can cause thread divergence on GPUs. In contrast, sampling from discrete distributions like the Rademacher or Uniform distribution is computationally inexpensive, as it maps directly to the native integer outputs of pseudo-random number generators via simple bitwise masking or linear scaling, bypassing the need for complex function evaluations.

Furthermore, the use of discrete noise—specifically Rademacher noise where  $E \in \{-1, +1\}$ —offers opportunities for hardware-level optimizations in the arithmetic logic units (ALUs). When the noise component is restricted to binary values, the matrix-vector multiplication associated with noise injection reduces from full floating-point operations (FLOPs) to conditional sign flips (additions and subtractions). For high-dimensional diffusion models deployed on resource-constrained edge devices, FPGAs, or specialized AI accelerators, eliminating these multiplication cycles can yield significant improvements in both latency and energy efficiency without requiring changes to the model weights.

To quantify the error introduced by this replacement, consider the one-step mean squared error:

$$\begin{aligned} \mathbb{E}\left[|\epsilon_t|^2\right] &= \sigma^2(\tau)\mathbb{E}\left[\left|B_h - \sqrt{h}E\right|^2\right] \\ &= \sigma^2(\tau)\left(\mathbb{E}[B_h^2] + \mathbb{E}[hE^2] - 2\mathbb{E}[B_h\sqrt{h}E]\right) \\ &= \sigma^2(\tau)(h + h - 2h\mathbb{E}[ZE]), \end{aligned}$$

where  $Z \sim \mathcal{N}(0, 1)$  and is independent of  $E$ . Since  $\mathbb{E}[ZE] = 0$  under independence, the one-step error simplifies to

$$\mathbb{E}\left[|\epsilon_t|^2\right] = 2\sigma^2(\tau)h.$$

Applying a discrete version of Grönwall’s inequality, we obtain the following bound on the total error:

$$\left( \mathbb{E} \left[ \sup_{0 \leq \tau \leq 1} \left| \overline{X}_\tau^{(h)} - \overline{X}'_\tau^{(h)} \right|^2 \right] \right)^{1/2} \leq Ch^{1/2},$$

for some constant  $C > 0$  depending on the drift and diffusion coefficients.

Combining this with the Euler–Maruyama error bound using the triangle inequality yields our main result:

**Theorem 3.2.** *Suppose there exists a constant  $k > 0$  such that*

$$\begin{aligned} |b(t, x) - b(s, y)| + |\sigma(t) - \sigma(s)| &\leq k \left( |x - y| + |t - s|^{1/2} \right), \\ |b(t, 0)| + |\sigma(t)| &\leq k, \end{aligned}$$

for all  $t, s \in [0, 1]$  and  $x, y \in \mathbb{R}$ . Then there exists a constant  $c = c(k, x) > 0$  such that

$$\left( \mathbb{E} \left[ \sup_{0 \leq t \leq 1} \left| \overline{X}'_t^{(h)} - \overline{X}_t \right|^2 \right] \right)^{1/2} \leq ch^{1/2}.$$

*Remark 3.3.* We provide some justification for the Lipschitz conditions. A central concept of diffusion models is that with sufficiently many timesteps in the learning phase (the forward direction of the SDE), the process converges to pure noise that no longer depends on the original dataset. For this to hold, we require

$$\prod_{t=1}^T (1 - \beta(t)) = \prod_{s=1}^T \left( 1 - \frac{1}{T} \sigma(sh) \right) \simeq 0.$$

If we assume that the above expression does not depend on  $T$ , then the Lipschitz condition for  $\sigma$  is preserved as  $T$  varies. For instance, in the linear schedule for  $\beta$ ,

$$\beta(t) = \beta_{\min}(T) + \frac{t}{T} (\beta_{\max}(T) - \beta_{\min}(T)),$$

maintaining the same scale of the product requires  $\beta_{\min}$  and  $\beta_{\max}$  to be proportional to  $1/T$ . This ensures that the Lipschitz condition of  $\sigma$  is preserved. In fact, in this case  $\sigma$  does not depend on  $T$ , and we can naturally establish convergence of the error rate.

To guarantee that the discretization error is at most  $\varepsilon$ , we require

$$ch^{1/2} \leq \varepsilon \quad \implies \quad h \leq \left( \frac{\varepsilon}{c} \right)^2.$$

Since  $h = 1/T$ , the number of discretization steps must satisfy  $T \geq \left( \frac{\varepsilon}{c} \right)^2$ . Thus, to achieve an  $\mathcal{O}(\varepsilon)$  strong error, it suffices to choose

$$T = \mathcal{O} \left( \frac{1}{\varepsilon^2} \right).$$

---

**Algorithm 1** Euler-Maruyama Sampling with Alternative Noise
 

---

**Input:** Score model  $\epsilon_\theta$ , noise schedule  $\sigma(\cdot)$ , number of steps  $T$ , noise distribution  $p_{noise}$  (e.g., Rademacher)  
**Output:** Sample  $\bar{X}_0$   
 Initialize  $\bar{X}_1 \sim \mathcal{N}(0, I)$   
 $h \leftarrow 1/T$   
**for**  $\tau = 1$  **down to**  $h$  **step**  $h$  **do**  
   Sample  $E \sim p_{noise}$  such that  $\mathbb{E}[E] = 0, \mathbb{V}[E] = 1$   
   Compute drift:  $d \leftarrow \left( \frac{\beta(\tau)}{\sigma(\tau)} \epsilon_\theta(\bar{X}_\tau, \tau) - \frac{\beta(\tau)}{2} \bar{X}_\tau \right)$   
   Update:  $\bar{X}_{\tau-h} \leftarrow \bar{X}_\tau - d \cdot h - \sigma(\tau) \sqrt{h} E$   
**end for**  
**return**  $\bar{X}_0$

---

### 3.3 Extension to the Multidimensional Case

In the multidimensional setting with dimension  $d$ , the analysis proceeds similarly. We consider  $d$  independent noise variables, and let  $E \in \mathbb{R}^d$  be a discrete random vector with mean zero and identity covariance, i.e.,  $\mathbb{E}[E] = 0, \mathbb{E}[EE^\top] = I_d$ . The modified update rule becomes

$$\bar{X}_{\tau-h}^{(h)} = \bar{X}_\tau^{(h)} - b\left(\bar{X}_\tau^{(h)}, \tau\right) h - \sigma(\tau) \sqrt{h} E,$$

where  $\sigma(\tau) \in \mathbb{R}^{d \times d}$ . The one-step mean squared error grows proportionally to  $h \cdot \text{Tr}(\sigma(\tau)\sigma(\tau)^\top)$ , and hence, by applying standard techniques including the discrete Grönwall inequality, we obtain the strong approximation error

$$\left( \mathbb{E} \left[ \sup_{0 \leq \tau \leq 1} \left\| \bar{X}_\tau^{(h)} - \bar{X}_\tau^{(h)} \right\|^2 \right] \right)^{1/2} \leq cd^{1/2} h^{1/2},$$

for some constant  $c > 0$  depending on the Lipschitz constants of  $b$  and  $\sigma$ , the initial condition, and the bound on the noise. In this setting, we therefore obtain the strong convergence rate  $d^{1/2} h^{1/2}$ . Thus, to achieve an  $\mathcal{O}(\varepsilon)$  strong error, the number of steps  $T$  must be chosen such that:

$$T = \mathcal{O} \left( \frac{d}{\varepsilon^2} \right).$$

For clarification, we restate our theorem below.

**Theorem 3.4.** *Consider the multi-dimensional VP-SDE*

$$d\bar{X}_\tau = b(\bar{X}_\tau, \tau) d\tau + \sigma(\tau) d\bar{W}_\tau$$

where  $\bar{X}_\tau \in \mathbb{R}^d$ ,  $b : \mathbb{R}^d \times [0, 1] \rightarrow \mathbb{R}^d$  and  $\sigma : [0, 1] \rightarrow \mathbb{R}^{d \times d}$ . Let

$$\bar{X}_\tau^{(h)} = \bar{X}_{sh}^{(h)} + b(\bar{X}_{sh}, sh) (\tau - sh) + \sigma(sh) (\bar{W}_\tau - \bar{W}_{sh}), \quad \tau \in [(s-1)h, sh].$$

be its Euler-Maruyama discretization. Suppose there exists  $k > 0$  such that

$$\begin{aligned} \|b(x, t) - b(y, s)\| + \|\sigma(t) - \sigma(s)\|_F &\leq k \left( \|x - y\| + |t - s|^{1/2} \right), \\ \|b(t, x)\| + \|\sigma(t, x)\|_F &\leq k \end{aligned}$$

for all time  $t, s$  and objectives  $x, y$ , where  $\|\cdot\|_F$  is the Frobenius norm. Then there exists  $c = c(k, x) > 0$  such that

$$\left( \mathbb{E} \left[ \sup_{0 \leq t \leq 1} \left\| \overline{X}_t^{(h)} - \overline{X}_t \right\|^2 \right] \right)^{1/2} \leq cd^{1/2}h^{1/2}.$$

*Proof.* Let  $[s] = \lfloor s/h \rfloor h$  denote the start of the discretization interval containing  $s$ . Then

$$\overline{X}_\tau^{(h)} - \overline{X}_\tau = \int_\tau^1 \underbrace{b\left(\overline{X}_{[s]}^{(h)}, [s]\right) - b\left(\overline{X}_s^{(h)}, s\right)}_{=A} ds + \int_\tau^1 \underbrace{b\left(\overline{X}_s^{(h)}, s\right) - b\left(\overline{X}_s, s\right)}_{=B} ds + \int_\tau^1 \underbrace{\sigma([s]) - \sigma(s)}_{=C} d\overline{W}_s.$$

Here, note that

$$\begin{aligned} \mathbb{E} [\|A\|^2] &\leq k^2 \left( |s - [s]|^{1/2} + \mathbb{E} \left[ \left\| \overline{X}_s^{(h)} - \overline{X}_{[s]}^{(h)} \right\| \right] \right)^2 \leq 2k^2 \left( |s - [s]| + \mathbb{E} \left[ \left\| \overline{X}_s^{(h)} - \overline{X}_{[s]}^{(h)} \right\|^2 \right] \right) \\ \mathbb{E} [\|B\|^2] &\leq k^2 \mathbb{E} \left[ \left\| \overline{X}_s^{(h)} - \overline{X}_s \right\|^2 \right]. \end{aligned}$$

We observe that the mean square displacement of the single step is small enough:

$$\mathbb{E} \left[ \left\| \overline{X}_s^{(h)} - \overline{X}_{[s]}^{(h)} \right\|^2 \right] \leq 2\mathbb{E} [\|b([s])\|^2 h^2] + 2\mathbb{E} [\|\sigma([s])\|_F^2 dh] \leq 2k^2 h^2 + 2k^2 dh.$$

By Itô isometry, we have

$$\mathbb{E} [\|C\|^2] = \int_\tau^1 \mathbb{E} [\|\sigma([s]) - \sigma(s)\|_F^2] ds \leq k^2 |s - [s]| \leq k^2 h.$$

By Jensen's inequality, we have

$$\begin{aligned} \mathbb{E} \left[ \sup_{x \leq \tau \leq 1} \left\| \int_\tau^1 A ds \right\|^2 \right] &\leq (1-x) \int_x^1 \mathbb{E} [\|A\|^2] ds, \\ \mathbb{E} \left[ \sup_{x \leq \tau \leq 1} \left\| \int_\tau^1 B ds \right\|^2 \right] &\leq (1-x) \int_x^1 \mathbb{E} [\|B\|^2] ds, \end{aligned}$$

Also, by Doob's maximal inequality, we have

$$\mathbb{E} \left[ \sup_{x \leq \tau \leq 1} \left\| \int_\tau^1 \sigma([s]) - \sigma(s) d\overline{W}_s \right\|^2 \right] \leq 4\mathbb{E} \left[ \int_x^1 \|\sigma([s]) - \sigma(s)\|_F^2 ds \right] \leq 4k^2 h.$$

Now, let

$$m(x) = \mathbb{E} \left[ \sup_{x \leq \tau \leq 1} \left\| \overline{X}_\tau^{(h)} - \overline{X}_\tau \right\|^2 \right].$$

Then

$$\begin{aligned}
m(x) &\leq 3 \left( \mathbb{E} \left[ \sup_{x \leq \tau \leq 1} \left\| \int_{\tau}^1 A ds \right\|^2 \right] + \mathbb{E} \left[ \sup_{x \leq \tau \leq 1} \left\| \int_{\tau}^1 B ds \right\|^2 \right] + 4 \mathbb{E} \left[ \int_x^1 \|\sigma([s]) - \sigma(s)\|_F^2 ds \right] \right) \\
&\leq 3 \left( (1-x) \int_x^1 \mathbb{E} [\|A\|^2] ds + (1-x) \int_x^1 \mathbb{E} [\|B\|^2] ds + 4 \int_x^1 \mathbb{E} [\|C\|^2] ds \right) \\
&\leq 6k^2 \int_x^1 |s - [s]| + \mathbb{E} \left[ \left\| \overline{X}_s^{(h)} - \overline{X}_{[s]}^{(h)} \right\|^2 \right] ds + 3k^2 \int_x^1 \mathbb{E} \left[ \left\| \overline{X}_s^{(h)} - \overline{X}_s \right\|^2 \right] ds + 12k^2 h \\
&\leq 6k^2 (h + 2k^2 h^2 + 2k^2 dh) + 3k^2 \int_x^1 m(s) ds + 12k^2 h \\
&\leq (12k^4 d + 18k^2 + 12k^4 h) h + 3k^2 \int_x^1 m(s) ds.
\end{aligned}$$

Hence, for some constant  $c = c(k) > 0$ ,

$$m(x) \leq cdh + c \int_x^1 m(s) ds.$$

Applying Grönwall's inequality, we obtain

$$m(x) \leq cdhe^{c(1-x)} \leq cdhe^c.$$

□

Theorem 3.4 establishes the  $O(h^{1/2})$  convergence rate for the Euler-Maruyama discretization under standard Gaussian increments, practical implementations often utilize discrete random variables to simulate noise. This raises the question of whether the convergence rate is preserved when the Gaussian assumption is relaxed. The following theorem addresses this by considering a process  $\overline{X}_t^{(h)}$  driven by general discrete noise, utilizing the result of Theorem 3.4 as a foundational bound.

**Theorem 3.5.** *Suppose there exists a constant  $k > 0$  such that*

$$\begin{aligned}
\|b(t, x) - b(s, y)\| + \|\sigma(t) - \sigma(s)\|_F &\leq k \left( \|x - y\| + |t - s|^{1/2} \right), \\
\|b(t, x)\| + \|\sigma(t)\|_F &\leq k,
\end{aligned}$$

for all  $t, s \in [0, 1]$  and  $x, y \in \mathbb{R}^d$ . Then there exists a constant  $C = C(k, x) > 0$  such that

$$\left( \mathbb{E} \left[ \sup_{0 \leq t \leq 1} \left\| \overline{X}_t^{(h)} - \overline{X}_t \right\|^2 \right] \right)^{1/2} \leq Cd^{1/2} h^{1/2}.$$

*Proof.* We aim to bound the error between the process driven by discrete noise,  $\overline{X}_t^{(h)}$ , and the true solution  $\overline{X}$ . By the triangle inequality:

$$\begin{aligned}
\left( \mathbb{E} \left[ \sup_{0 \leq t \leq 1} \left| \overline{X}_t^{(h)} - \overline{X}_t \right|^2 \right] \right)^{1/2} &\leq \underbrace{\left( \mathbb{E} \left[ \sup_{0 \leq t \leq 1} \left| \overline{X}_t^{(h)} - \overline{X}_t^{(h)} \right|^2 \right] \right)^{1/2}}_{(I: \text{Noise Coupling (via KMT)})} \\
&\quad + \underbrace{\left( \mathbb{E} \left[ \sup_{0 \leq t \leq 1} \left| \overline{X}_t^{(h)} - \overline{X}_t \right|^2 \right] \right)^{1/2}}_{(II: \text{Result from Theorem 3.4})}.
\end{aligned}$$

From Theorem 3.4), we have established that  $(II) \leq c_1 d^{1/2} h^{1/2}$ . We now focus on bounding  $(I)$ , the distance between the Euler-Maruyama approximation driven by Gaussian noise ( $W$ ) and the one driven by discrete noise ( $E$ ). The discretized processes satisfy:

$$\begin{aligned}\overline{X}_{k+1}^{(h)} &= \overline{X}_k^{(h)} + b(\overline{X}_k^{(h)})h + \sigma(kh)\Delta W_k, \quad \text{where } \Delta W_k \sim \mathcal{N}(0, hI_d) \\ \overline{X}'_{k+1}^{(h)} &= \overline{X}'_k^{(h)} + b(\overline{X}'_k^{(h)})h + \sigma(kh)\sqrt{h}E_k, \quad \text{where } \mathbb{E}[E_k] = 0, \text{Cov}[E_k] = I_d.\end{aligned}$$

A crucial result in probability theory (the Skorokhod embedding theorem or the KMT approximation) states that for a random walk  $S_n = \sum_{i=1}^n E_i$  with zero mean and finite moments, one can construct a Brownian motion  $W$  on the same probability space such that the partial sums approximate the Brownian path. Specifically, there exists a coupling such that:

$$\mathbb{E} \left[ \sup_{0 \leq k \leq 1/h} \left\| \sum_{i=0}^{k-1} \sqrt{h}E_i - W_{kh} \right\|^2 \right] \leq C_E dh$$

for some constant  $C_E$ . Let  $M_k = \sum_{i=0}^{k-1} \sqrt{h}E_i$  and  $W_k = W_{kh}$ . The difference between the noise paths is small.

Let  $\delta_k = \overline{X}'_k^{(h)} - \overline{X}_k^{(h)}$ . Subtracting the update equations:

$$\delta_{k+1} = \delta_k + \left( b(\overline{X}'_k^{(h)}) - b(\overline{X}_k^{(h)}) \right) h + \sigma(kh)(\sqrt{h}E_k - \Delta W_k).$$

We can rewrite the noise term accumulation. Let  $Z_k = \sum_{i=0}^{k-1} (\sqrt{h}E_i - \Delta W_i)$  be the difference in the driving noise paths. Summing the recurrence:

$$\delta_n = \sum_{k=0}^{n-1} \left( b(\overline{X}'_k^{(h)}) - b(\overline{X}_k^{(h)}) \right) h + \sum_{k=0}^{n-1} \sigma(kh)(\sqrt{h}E_k - \Delta W_k).$$

Using summation by parts (Abel transformation) on the noise term:

$$\sum_{k=0}^{n-1} \sigma(kh)(Z_{k+1} - Z_k) = \sigma((n-1)h)Z_n - \sum_{k=0}^{n-1} (\sigma(kh) - \sigma((k-1)h))Z_k.$$

Using the Lipschitz bound on  $\sigma$  and  $b$ , and the noise approximation bound  $\mathbb{E}[\sup \|Z_k\|^2] \leq Cdh$ , we proceed. Taking norms and expectations:

$$\|\delta_n\| \leq h \sum_{k=0}^{n-1} k_L \|\delta_k\| + \|\text{NoiseTerm}_n\|.$$

Squaring and using Cauchy-Schwarz:

$$\|\delta_n\|^2 \leq C \left( \sum_{k=0}^{n-1} \|\delta_k\|^2 h + \sup_k \|Z_k\|^2 \right).$$

Applying the discrete Grönwall inequality:

$$\sup_n \mathbb{E}[\|\delta_n\|^2] \leq C \mathbb{E} \left[ \sup_k \|Z_k\|^2 \right] \exp(C).$$

Since  $\mathbb{E}[\sup \|Z_k\|^2] \leq \mathcal{O}(dh)$  via the embedding theorem:

$$\left( \mathbb{E} \left[ \sup_{0 \leq t \leq 1} \left\| \overline{X}'_t^{(h)} - \overline{X}_t^{(h)} \right\|^2 \right] \right)^{1/2} \leq Cd^{1/2}h^{1/2}.$$

Combining this with term  $(II)$ , the total error is bounded by  $(C + c_1)d^{1/2}h^{1/2}$ .  $\square$

## 4 EXPERIMENTS

All experiments were conducted on a personal computer equipped with an NVIDIA RTX 4070 GPU. We evaluate noise substitution and zigzag sampling in diffusion models through a series of experiments. Figures 1 and 3 illustrate representative sample results, highlighting how noise type and noise scaling influence generation quality.

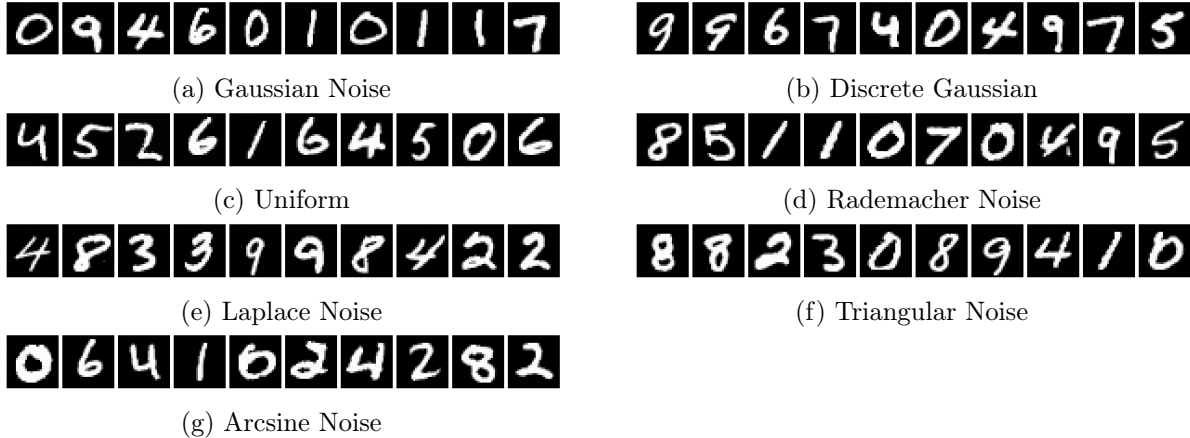


Figure 1: MNIST Image Samples with Various Noises

### 4.1 Performance of Various Noises

Table 1: FID Scores with Various Noises

NOISE	FID(MNIST)	FID(CIFAR-10)
Gaussian	2.994326	14.642573
Discrete Gaussian	3.005654	14.672305
Uniform	2.972102	14.592020
Rademacher	2.987234	14.540516
Laplace	5.766727	34.587563
Triangular	2.960605	14.503871
Arcsine	2.987144	14.631359

**Setup:** We evaluate how different noise distributions affect the sampling quality of a Denoising Diffusion Probabilistic Model (DDPM) trained on the MNIST and CIFAR10 dataset. We test several symmetric noise distributions—Gaussian, Uniform, Rademacher, Triangular, Arcsine—and one asymmetric distribution, Laplace. All noises are scaled to have zero mean and unit variance to match the standard Gaussian noise used in training. Additionally, we include Discrete Gaussian noise, a discrete random variable whose probability mass function is proportional to the probability density of a standard normal distribution evaluated at integer points. Sample quality is assessed using the Fréchet Inception Distance (FID) score.

**Result:** The empirical results, summarized in Table 1, demonstrate that most symmetric noise distributions produce sample quality comparable to standard Gaussian noise across both datasets.

On MNIST, the FID scores for Uniform, Rademacher, Triangular, and Arcsine noise are all within a negligible margin of the Gaussian baseline. This trend holds for the more complex CIFAR-10 dataset, where Rademacher and Arcsine noise achieve parity with Gaussian noise (e.g., 14.54 vs. 14.64). We note that the absolute FID scores for CIFAR-10 are higher than current state-of-the-art benchmarks. This is because we employed a lightweight model architecture and a fixed, limited training budget to facilitate a broad ablation study on academic hardware. However, the key finding is the relative performance consistency: the substitution of Gaussian noise with computationally cheaper symmetric alternatives does not degrade generation quality. In contrast, the Laplace distribution—the only asymmetric noise tested—resulted in significantly higher FID scores on both datasets (5.77 on MNIST and 34.59 on CIFAR-10), confirming that while the specific shape of the distribution is flexible, symmetry is a critical property for minimizing discretization error.

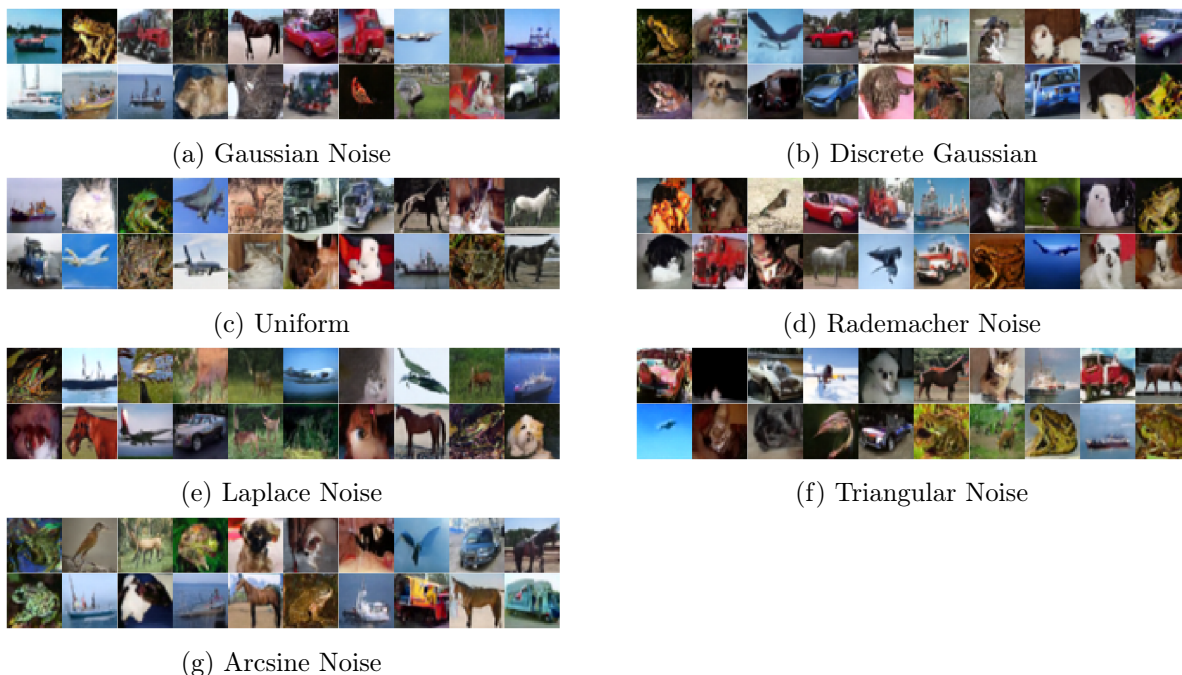


Figure 2: CIFAR-10 Image Samples with Various Noises

## 4.2 Noise Scale Ablation

**Setup:** To study the effect of noise variance on sample quality, we conducted an ablation study replacing standard Gaussian noise with a Rademacher distribution, where components are drawn from  $\{-\alpha, \alpha\}$ . This setup provides direct control over the variance through the scalar  $\alpha$  while preserving the zero-mean and symmetric properties of the noise. We evaluated generated samples using the Fréchet Inception Distance (FID) across a range of  $\alpha$  values, hypothesizing an optimum at  $\alpha = 1.0$  to match the unit variance of the training noise.

**Result:** The results in Table 2 confirm that noise variance is critical to the synthesis process. The FID score exhibits a sharp, convex relationship with the noise scale  $\alpha$ , reaching a minimum at the hypothesized optimum of  $\alpha = 1.0$ . Insufficient variance ( $\alpha < 1.0$ ) leads to mode collapse and blurry images, whereas excessive variance ( $\alpha > 1.0$ ) results in residual noise and artifacts. These findings confirm that matching the statistical moments of the sampling noise to the training distribution is essential for high-fidelity generation.

Table 2: Sampling with Scaled Rademacher Noise

NOISE SCALE	FID SCORE
0.1	97.936673
0.2	77.937531
0.4	47.992128
0.8	11.771176
0.9	6.159960
1.0	2.987234
1.1	4.307226
1.2	12.735438
1.3	30.257889
1.5	90.242229

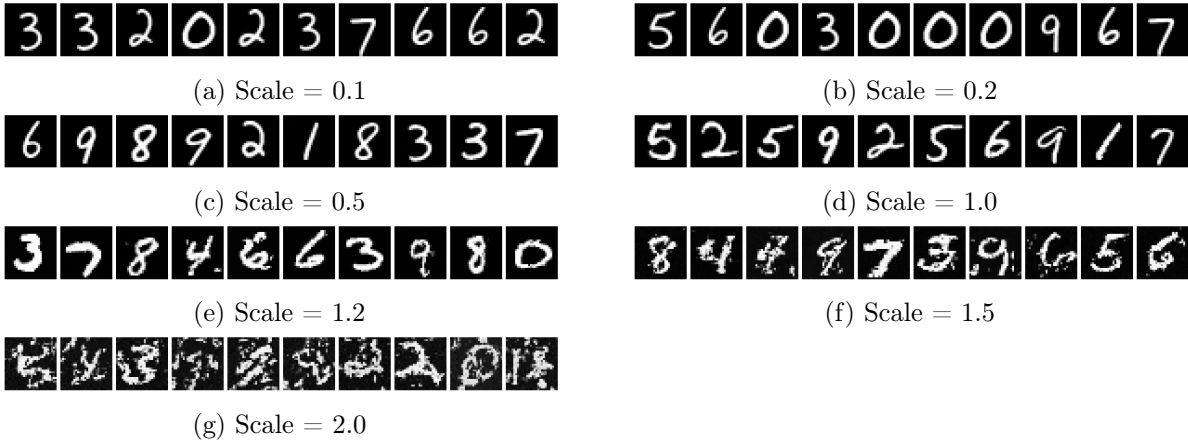


Figure 3: Image Samples with Scaled Rademacher Noise

## 5 DISCUSSION

In this work, we presented a rigorous yet simplified analysis of the Euler–Maruyama discretization error for sampling in diffusion models. By utilizing a time-rescaling approach and Grönwall’s inequality, we established a strong convergence rate of  $\mathcal{O}(1/\sqrt{T})$  under standard Lipschitz continuity assumptions. This framework offers a more accessible alternative to existing complex proofs, facilitating future theoretical explorations into the convergence properties of generative SDEs.

A key contribution of our study is the theoretical and empirical validation of noise substitution. We demonstrated that the standard Gaussian noise in the reverse process can be replaced by computationally cheaper discrete alternatives, such as Rademacher or Uniform noise, without compromising the convergence rate or sample quality. This interchangeability has profound implications for the deployment of diffusion models on resource-constrained hardware. By eliminating the need for expensive Gaussian random number generators (RNGs) and enabling the use of simple bitwise operations or integer arithmetic for noise injection, our findings pave the way for highly efficient FPGA and mobile-edge implementations.

Furthermore, our results shed light on the fundamental robustness of the diffusion sampling

process. The empirical parity between Gaussian and symmetric discrete noises—observed across both MNIST and CIFAR-10 datasets—suggests that the generative capability of these models is driven primarily by the first two moments of the driving noise process, rather than the specific shape of the distribution. This aligns with the "universality" often seen in high-dimensional probability theory. However, the degradation observed with asymmetric noise (Laplace) highlights a critical boundary condition: while the distribution shape is flexible, symmetry remains a necessary condition for minimizing discretization error in the standard VP-SDE formulation.

Future work may extend this analysis to lower-precision quantization regimes, exploring the limits of noise simplification before the model’s performance deteriorates. Furthermore, applying this simplified proof technique to other SDE-based paradigms, such as Consistency Models or Flow Matching, presents a promising direction for unifying the theoretical landscape of generative modeling.

## Acknowledgements

This work was supported by the New Faculty Startup Fund from Seoul National University.

## References

- Arpit Bansal, Eitan Borgnia, Hong-Min Chu, Jie S Li, Hamid Kazemi, Furong Huang, Micah Goldblum, Jonas Geiping, and Tom Goldstein. Cold diffusion: Inverting arbitrary image transforms without noise. In *Proceedings of the IEEE/CVF Conference on Computer Vision and Pattern Recognition*, 2022.
- Joe Benton, Valentin De Bortoli, Arnaud Doucet, and George Deligiannidis. Nearly  $d$ -linear convergence bounds for diffusion models via stochastic localization. In *The Twelfth International Conference on Learning Representations (ICLR)*, 2023.
- Hongrui Chen, Holden Lee, and Jianfeng Lu. Improved analysis of score-based generative modeling: User-friendly bounds under minimal smoothness assumptions. In *Proceedings of the 40th International Conference on Machine Learning*, volume 202, pages 4735–4763. PMLR, 2023a. URL <https://proceedings.mlr.press/v202/chen23q.html>.
- Sitan Chen, Sinho Chewi, Jungshian Li, Yuanzhi Li, Adil Salim, and Anru R. Zhang. Sampling is as easy as learning the score: Theory for diffusion models with minimal data assumptions. In *Proceedings of the 11th International Conference on Learning Representations (ICLR)*, 2023b.
- Giannis Daras, Mauricio Delbracio, Hossein Talebi, Alexandros G Dimakis, and Peyman Milanfar. Soft diffusion: Score matching for general corruptions. In *Advances in Neural Information Processing Systems*, volume 35, 2022.
- Ian J. Goodfellow, Jean Pouget-Abadie, Mehdi Mirza, Bing Xu, David Warde-Farley, Sherjil Ozair, Aaron C. Courville, and Yoshua Bengio. Generative adversarial nets. In *Advances in Neural Information Processing Systems 27: Annual Conference on Neural Information Processing Systems 2014, December 8-13 2014, Montreal, Quebec, Canada*, pages 2672–2680, 2014.
- T. H. Gronwall. Note on the derivatives with respect to a parameter of the solutions of a system of differential equations. *Annals of Mathematics*, 20(4):292–296, 1919. ISSN 0003486X, 19398980. URL <http://www.jstor.org/stable/1967124>.

- Jonathan Ho, Ajay Jain, and Pieter Abbeel. Denoising diffusion probabilistic models. In *Advances in Neural Information Processing Systems*, volume 33, pages 6840–6851, 2020.
- Jonathan Ho, Tim Salimans, William Chan, Prajit Ramachandran, and Xi Chen. Classifier-free diffusion guidance. *arXiv preprint arXiv:2207.12598*, 2022a.
- Jonathan Ho et al. Imagen video: High definition video generation with diffusion models. *arXiv preprint arXiv:2210.02303*, 2022b.
- Yuchen Jiao and Gen Li. Instance-dependent convergence theory for diffusion models. *arXiv preprint arXiv:2410.13738*, 2025. URL <https://doi.org/10.48550/arXiv.2410.13738>.
- Diederik P. Kingma and Max Welling. Auto-encoding variational bayes. In Yoshua Bengio and Yann LeCun, editors, *2nd International Conference on Learning Representations, ICLR 2014, Banff, AB, Canada, April 14-16, 2014, Conference Track Proceedings*, 2014.
- Zhifeng Kong, Wei Ping, Jiaji Huang, Kexin Zhao, and Bryan Catanzaro. Diffwave: A versatile diffusion model for audio synthesis. In *International Conference on Learning Representations (ICLR)*, 2021.
- Holden Lee, Jianfeng Lu, and Yixin Tan. Convergence of score-based generative modeling for general data distributions. In *Proceedings of the 34th International Conference on Algorithmic Learning Theory (ALT)*, 2023. URL <https://arxiv.org/abs/2209.12381>.
- Gen Li, Yuting Wei, Yuxin Chen, and Yuejie Chi. Towards faster non-asymptotic convergence for diffusion-based generative models. *arXiv preprint arXiv:2306.09251*, 2023. URL <https://arxiv.org/abs/2306.09251>.
- Gen Li, Yuting Wei, Yuejie Chi, and Yuxin Chen. A sharp convergence theory for the probability flow odes of diffusion models. *arXiv preprint arXiv:2408.02320*, 2024. URL <https://arxiv.org/abs/2408.02320>. 2024c.
- Robin Nachmani, Eliya and Romanowitz and Lior Wolf. Denoising diffusion gamma models. In *International Conference on Learning Representations*, 2021.
- V Pandey et al. Heavy-tailed diffusion models. In *International Conference on Learning Representations*, 2025.
- Aditya Ramesh, Prafulla Dhariwal, Alex Nichol, Casey Chu, and Mark Chen. Hierarchical text-conditional image generation with clip latents. *arXiv preprint arXiv:2204.06125*, 2022.
- Chitwan Saharia, William Chan, Saurabh Saxena, Lala Li, Jay Whang, Emily Denton, Tim Salimans, Jonathan Ho, David J Fleet, and Mohammad Norouzi. Photorealistic text-to-image diffusion models with deep language understanding. In *Advances in Neural Information Processing Systems*, 2022.
- Jascha Sohl-Dickstein, Eric Weiss, Niru Maheswaranathan, and Surya Ganguli. Deep unsupervised learning using nonequilibrium thermodynamics. In *International Conference on Machine Learning*, pages 2256–2265. PMLR, 2015.
- Jiaming Song, Chenlin Meng, and Stefano Ermon. Denoising diffusion implicit models. In *International Conference on Learning Representations*, 2021a.

- Yang Song, Jascha Sohl-Dickstein, Diederik Kingma, Abhishek Kumar, Stefano Ermon, and Ben Poole. Score-based generative modeling through stochastic differential equations. *ICLR*, 2021b.
- Yang Song, Prafulla Dhariwal, Mark Chen, and Ilya Sutskever. Consistency models. In Andreas Krause, Emma Brunskill, Kyunghyun Cho, Barbara Engelhardt, Sivan Sabato, and Jonathan Scarlett, editors, *Proceedings of the 40th International Conference on Machine Learning*, volume 202 of *Proceedings of Machine Learning Research*, pages 32211–32252. PMLR, 23–29 Jul 2023. URL <https://proceedings.mlr.press/v202/song23a.html>.
- W. Tang and H. Zhao. Score-based diffusion models via stochastic differential equations—a technical tutorial. *arXiv preprint arXiv:2402.07487*, 2024. URL <https://arxiv.org/abs/2402.07487>.
- Brian L. Trippe et al. Diffusion probabilistic modeling of protein backbones in 3d for the motif-scaffolding problem. *arXiv preprint arXiv:2206.04119*, 2022.
- James L. Watson et al. De novo design of protein structure and function with rfdiffusion. *Nature*, 620(7975):824–831, 2023.
- Julia Wolleb, Luc Van Gool, Jonas Schmid, Christos Davatzikos, Sinan Candemir, and Martin Sandkühler. Diffusion models for medical anomaly detection. *arXiv preprint arXiv:2203.04391*, 2022.
- Lin Xiao, Chenlin Meng, Yang Song, and Stefano Ermon. On discrete denoising score matching for practical learning of diffusion models. In *Advances in Neural Information Processing Systems (NeurIPS)*, 2022.
- L. Yang, Z. Zhang, Y. Song, S. Hong, R. Xu, Y. Zhao, W. Zhang, B. Cui, and M.-H. Yang. Diffusion models: A comprehensive survey of methods and applications. *ACM Computing Surveys*, 56(4): 1–39, 2023.
- Hyeongju Yoon, Eunwoo Park, and Ernest K Ryu. Score-based generative models with Lévy processes. In *Advances in Neural Information Processing Systems*, volume 36, 2023.

# A EXPERIMENT SETTINGS

## A.1 Performance of Various Noises

The alternative noises used in our experiments are defined as below. `torch` and `math` modules are used.

```
1 def DG_matrix(shape, device = None):
2     if device is None:
3         device = torch.device('cuda' if torch.cuda.is_available() else 'cpu')
4         probs = torch.rand(shape, device = device)
5         matrix = torch.zeros_like(probs)
6
7         sqrt3 = math.sqrt(3)
8         matrix[probs < 1/6] = -sqrt3
9         matrix[(probs >= 1/6) & (probs < 1/3)] = sqrt3
10        return matrix
```

Listing 1: Discrete Gaussian Noise

```
1 def UD_matrix(shape, device=None):
2     if device is None:
3         device = torch.device('cuda' if torch.cuda.is_available() else 'cpu')
4
5     a = -math.sqrt(3)
6     b = math.sqrt(3)
7
8     matrix = torch.empty(shape, device=device).uniform_(a, b)
9     return matrix
```

Listing 2: Uniform Noise

```
1 def Rademacher_matrix(shape, device=None):
2     if device is None:
3         device = torch.device('cuda' if torch.cuda.is_available() else 'cpu')
4     matrix = 2 * torch.randint(0, 2, shape, device=device).float() - 1
5     return matrix
```

Listing 3: Rademacher Noise

```
1 def Laplace_matrix(shape, device=None):
2     if device is None:
3         device = torch.device('cuda' if torch.cuda.is_available() else 'cpu')
4     b = 1 / math.sqrt(2)
5     u = torch.rand(shape, device=device) - 0.5
6     matrix = -b * torch.sign(u) * torch.log1p(-2 * u.abs())
7     return matrix
```

Listing 4: Laplace Noise

```
1 def Triangular_matrix(shape, device=None):
2     if device is None:
3         device = torch.device('cuda' if torch.cuda.is_available() else 'cpu')
4     a = -math.sqrt(6)
5     b = 0
6     c = math.sqrt(6)
7     u = torch.rand(shape, device=device)
8     matrix = torch.where(
9         u < (b - a) / (c - a),
```

```

10     a + torch.sqrt(u * (b - a) * (c - a)),
11     c - torch.sqrt((1 - u) * (c - b) * (c - a))
12 )
13 return matrix

```

Listing 5: Triangular Noise

```

1 def Arcsine_matrix(shape, device=None):
2     if device is None:
3         device = torch.device('cuda' if torch.cuda.is_available() else 'cpu')
4     u = torch.rand(shape, device=device)
5     matrix = math.sqrt(2) * torch.sin(math.pi * (u - 0.5))
6     return matrix

```

Listing 6: Arcsine Noise

## A.2 Evaluation

The evaluation of each experiments are done using Frécht Inception Distance (FID) score and CLIP-Maximum Mean Discrepancy (CMMD) score. For FID score evaluation, we used the `compute_fid` function in `cleanfid` module. We used `CLIPModel` and `CLIPProcessor` in `transformer` module to extract CLIP features from images and compute CMMD score.